



Research Article

Efficacy of Cetuximab and 4-PBA Combination Therapy in Human Oral Squamous Cell Carcinoma Cells

Akira Noguchi*, Takeshi Nishida, Hideki Hatta, Kohji Takagi, Toshiko Kakiuchi, Shinichi Tanaka, Takashi Minamisaka, Takahiko Nakajima, Johji Imura

Department of Diagnostic Pathology, Faculty of Medicine, Academic Assembly, University of Toyama, Toyama City, Japan

***Corresponding Author:** Akira Noguchi, Department of Diagnostic Pathology, Faculty of Medicine, Academic Assembly, University of Toyama, 2630 Sugitani, Toyama City, Toyama, 930-0194, Japan, Tel: +81764342281

Received: 23 November 2021; **Accepted:** 02 December 2021; **Published:** 20 December 2021

Citation: Akira Noguchi, Takeshi Nishida, Hideki Hatta, Kohji Takagi, Toshiko Kakiuchi, Shinichi Tanaka, Takashi Minamisaka, Takahiko Nakajima and Johji Imura. Efficacy of Cetuximab and 4-PBA Combination Therapy in Human Oral Squamous Cell Carcinoma Cells. Journal of Cancer Science and Clinical Therapeutics 5 (2021): 562-575.

Abstract

Cetuximab is a powerful anti-neoplastic agent that can inhibit cell growth in oral squamous cell carcinomas (OSCCs). Unfortunately, there are cases with unfavorable outcomes. Because few studies have focused on the combined effects of cetuximab and histone deacetylase (HDAC) inhibitors, we aimed to evaluate the antitumor effect of cetuximab in combination with HDAC inhibitors in human OSCC cell lines, and investigate the mechanism of apoptosis enhancing activity thereof. We used human OSCC cell lines treated with cetuximab and several HDAC

inhibitors. The WST assay and ApoToxGlo™ Triplex Assay determined cell survival. We employed the TdT-mediated dUTP-biotin nick end labeling method to detect apoptosis. We used western blotting to examine the histone acetylation status, ER stress markers, and epidermal growth factor receptor (EGFR) signaling pathways. Our results show that cetuximab in combination with 4-phenyl butyric acid (4-PBA) remarkably decreases cell growth in vitro. In addition, the combined treatment resulted in increased EGFR mRNA expression and promoted the activation of

ERK. The combination treatment induced apoptosis at a significantly higher frequency than did either agent alone. In conclusion, the combination of cetuximab and 4-PBA is more effective against human OSCC cells, allowing for potential clinical applicability of combination treatment in OSCC therapies.

Keywords: Oral squamous cell carcinoma; Combination therapy; Tetuximab; Histone deacetylase inhibitors; Cancer; Epigenetics

Abbreviations: CHOP - CCAAT/enhancer-binding protein homologous protein; EGFR - Epidermal growth factor receptor; MAPK - Mitogen-activated protein kinase; OSCC - Oral squamous cell carcinoma; HDAC - Histone deacetylase; HDACi - Histone deacetylase inhibitors; 4-PBA - 4-phenyl butyric acid; TUNEL - TdT-mediated dUTP-biotin nick end labeling; ACA-28 - Acetoxychavicol acetate-28; PCR - polymerase chain reaction

1. Introduction

Oral squamous cell carcinoma (OSCC) is a cancer originating from the oral mucosal epithelium that accounts for more than 90% of malignant tumors of the oral cavity and considerably influences the quality of life. Smoking is the predominant cause of OSCC [1] although, viruses such as human papillomavirus, particularly type 16, are thought to play a role in OSCC development [2]. At the cellular level, tumor suppressors (p53 and p16) are often lost whereas oncogenes, including epidermal growth factor receptor (EGFR) are amplified or mutated. Increased EGFR gene copy numbers and protein overexpression result from regulatory pathway changes, gene structure changes, or gene amplification, and these play an important role in carcinogenesis [3]. EGFR is an important therapeutic target

and prognostic factor for OSCC treatment. Treatment with the monoclonal antibody cetuximab exerts beneficial clinical effects. Cetuximab specifically binds to and degrades EGFR. In addition, cetuximab inhibits the binding of EGFR to its ligands and blocks the downstream signal transduction pathways, leading to inhibition of proliferation and apoptosis induction in tumor cells [4]. *RAS* somatic mutations are negative predictors of the clinical efficacy of anti-EGFR antibodies. Therefore, routine screening for mutations in *K-RAS* is used in colorectal cancer for patient selection prior to treatment [5, 6]. However, in OSCC, primary *RAS* mutations are rare and the importance of the mutations remain unclear [7, 8].

Epigenetic DNA and histone modifications alter chromatin conformation and play a predominant role in the control of transcription and regulation of genes. Histone deacetylases (HDACs) are powerful epigenetic regulators that act as transcriptional repressors by removing acetyl groups from histones. HDACs are dysregulated in many cancers, including OSCC, making them a therapeutic target for the treatment of cancer [9]. However, experimental and clinical studies have demonstrated that the currently available histone deacetylase inhibitors (HDACi) are not adequate as single-agent therapies against OSCC [9, 10], despite the fact that HDACi exert significant antitumor effects in combination therapies. The combination of HDACi with other standard chemotherapeutic agents could achieve higher anticancer effects in OSCC [11, 12]. Based on these reports, we hypothesized that cetuximab sensitivity is caused by the presence of epigenetic alterations and the approaches employed to screen candidate materials for repurposing and/or repositioning cetuximab in commercially available HDACi. Therefore, we investigated whether HDACi have a beneficial effect when combined with cetux-

imab in OSCC cells expressing high levels of EGFR.

2. Methods

2.1 Cell culture

B88 and KOSC-2 cells are human squamous cell carcinoma (SCC) cell lines established from SCCs of the tongue [13]. B88 was a generous gift from the Kanagawa Cancer Center Research Institute (Kanagawa, Japan). KOSC-2 was purchased from the JCRB Cell Bank (Osaka, Japan). In this study, both cells were routinely cultured in RPMI-1640 (Gibco Invitrogen, Carlsbad, CA, USA) supplemented with 10% fetal bovine serum, penicillin (100 U/ml), and streptomycin (100 µg/ml). Cultures were maintained in a humidified incubator at 37°C in 5% CO₂.

2.2 HDACi screening

Drug screening was performed using the DiscoveryPak HDAC Inhibitor Set (splitomicin, apicidin, valproic acid, trichostatin A, 4-phenyl butyric acid [4-PBA]) obtained from BioVision (Milpitas, CA, USA). Cetuximab was purchased from Merck Serono (Burlington, MA, USA). B88 and KOSC-2 cells were plated at 10,000 cells/well in a 96-well plate. After incubation for 24 h, HDACi, cetuximab (500 mg/ml), or both were added. After 24 h of incubation, the cell toxicity was evaluated using a Cell Counting Kit-8 assay (Dojindo Laboratories, Kumamoto, Japan). Absorbance at 450 nm was measured using a microplate reader (Thermo Scientific Multiskan FC, Thermo Fisher Scientific Life Sciences, Waltham, MA, USA).

2.3 RNA extraction and quantitative RT-PCR

The EGFR mRNA levels were determined at 24 h and 48 h post-treatment with 4-PBA (5 mM), cetuximab (500 mg/ml), or both by RT-qPCR. Total RNA was extracted from B88 cells using TRIzol reagent (Invitrogen, La Jolla,

CA, USA) according to the manufacturer's protocol. Two micrograms of cellular RNA were converted to cDNA following the manufacturer's instructions for the specific reverse transcription kit (Invitrogen). Quantitative RT-PCR was performed using primers specific for EGFR (Forward: 5'-AAGTGTAAGAAGTGCGAAGG-3'. Reverse: 5'-GGAGGAGTATGTGTGAAGGA-3'). The degree of expression was quantified using a relative standard curve and normalized to GAPDH that was amplified using specific primers (Forward: 5'-GTCAACGGATTGGTCGTATT-3'. Reverse: 5'-GATCTCGCTCCTGGAAGATGG-3').

2.4 Cell viability, cytotoxicity, and caspase 3/7 activities

Cell viability and caspase 3/7 activities were evaluated in B88 cells treated with 4-PBA (5 mM), cetuximab (500 mg/ml), or both using the ApoToxGlo Triplex Assay kit (Promega, Madison, WI, USA) following the manufacturer's instructions. The ApoToxGlo Triplex Assay combines three assay chemistries to assess viability, cytotoxicity, and caspase activation events in the same cell-based assay. Briefly, 10 µl of viability/cytotoxicity reagent containing both GF-AFC substrate and bis-AAF-R110 substrates were added to all wells. After incubation for 1 h at 37°C, the Relative Fluorescence Units (RFU) was determined at 370 Ex/535 Em for cell viability and at 485 Ex/535 Em for cytotoxicity. To determine the effect on caspase-3/7 activity of B88 cells treated with 4-PBA and cetuximab, 10 µl of luminogenic caspase-3/7 substrate, which contains the tetrapeptide sequence DEVD were added to all wells. The Relative Luminescence Units (RLU) from the caspase-3/7 activated was measured after 30 min of incubation. The fluorescence and luminescence were detected using a FilterMax-F5 (Molecular Devices LLC, Sunnyvale, CA, USA).

2.5 TdT-mediated dUTP-biotin nick end labeling assay

For the *in situ* analysis of DNA fragmentation, TdT-mediated dUTP-biotin nick end labeling (TUNEL) staining was performed using an ApopTag peroxidase in situ apoptosis detection kit (Merck Millipore, MA, USA) according to the manufacturer's instructions. The apoptotic index (average percentage of apoptotic cells labeled by the TUNEL method) was determined as the number of DAB-stained cells versus the total number of cells using light microscopy. A minimum of 1,000 cells were counted in random fields.

2.6 Western blot

Cells were lysed in a radioimmunoprecipitation assay buffer 24 h after drug treatment. The protein concentration was measured using a bicinchoninic acid protein assay kit (Thermo Fisher Scientific, Rockford, IL, USA). Samples were run on sodium dodecyl sulfate-polyacrylamide gel and transferred onto polyvinylidene difluoride membranes. After blocking with 5% skim milk, the membranes were incubated with primary antibodies. Blots were then incubated with peroxidase-conjugated secondary antibodies and detected by ECL chemiluminescence, and images were captured with ImageQuant LAS-500 analyzer (GE Healthcare Life Sciences, Pittsburgh, PA, USA).

Primary antibodies against the following proteins were used: EGFR, p-EGFR, ERK, Akt, p-AKT, cleaved-PARP, and GRP78 (Santa Cruz Biotechnologies, Santa Cruz, CA, USA); B-cell lymphoma 2 (bcl-2), CCAAT/enhancer-binding protein homologous protein (CHOP), and p-ERK (Cell Signaling Technology, Beverly, MA, USA); H3K9,14ac, H3K27ac, and H4K16ac (MAB Institute, Nagano, Japan); β -actin (Sigma-Aldrich, St. Louis, MO, USA).

2.7 Statistical analysis

All experiments were performed in triplicate and the values represent the average of at least three independent experiments. We expressed all data as mean \pm standard deviation. One-way analysis of variance (ANOVA) with Bonferroni's post-hoc test was used to analyze the differences between the combination of cetuximab and HDACi vs. individual treatments. *p* Values <0.05 were considered significant. We used SPSS software for Windows (V26.0; SPSS Inc., Chicago, IL, USA) for all statistical analyses.

3. Results

3.1 Effect of the combination of HDACi and Cetuximab in OSCC cell proliferation

To investigate the effect of HDACi in OSCC cells, B88 and KOSC-2 cells were treated with cetuximab, HDACi (200nM trichostatin A, 5mM 4-PBA, 60 μ M splitomicin, 50nM apicidin, 1mM valproic acid), or the combination of cetuximab and HDACi. Both cells showed similar findings. The cetuximab-treated group was slightly differentiated from the control group. When cells were treated with 4-PBA and trichostatin A, significant toxicity was observed (Figure 1A and B). Moreover, when treated with the combination, additive or synergistic action was observed. No difference was observed in splitomicin, apicidin, and valproic acid (Figure 1C-E). The results indicated 4-PBA as the most useful HDACi.

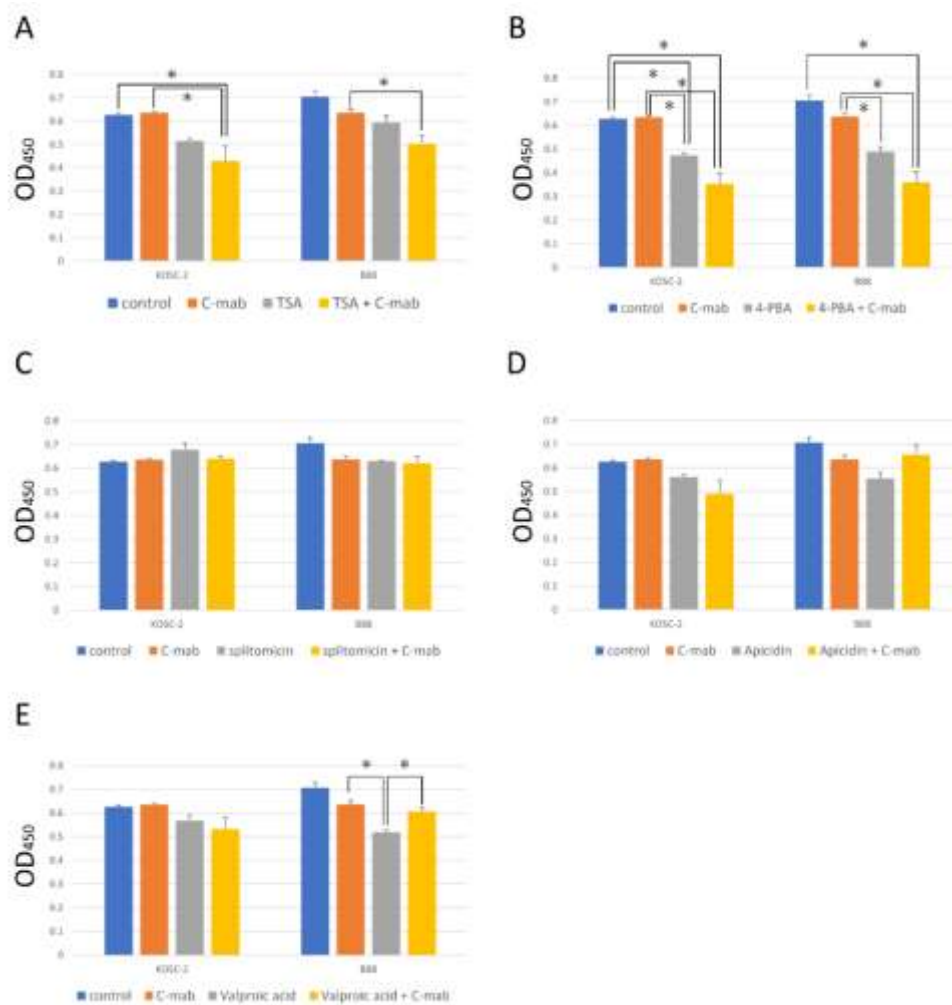


Figure 1: Cetuximab resistance cells were improved susceptibility of cetuximab by treatment with 4-PBA. KOSC-2 and B88 cells were treated with cetuximab and/or HDACi [trichostatin A (A), 4-PBA (B), splitomicin (C), apicidin (D), valproic acid (E)] for 24 h. The effect of cetuximab and/or HDACi on cell proliferation as measured by cell counting kit-8 assay. 4-PBA was most useful in HDACi. Values represent the mean \pm SD of three independent experiments. * $p < 0.05$.

3.2 Morphological changes in B88 cells after exposure to 4-PBA and/or cetuximab

B88 cells have an epithelial sheet-like structure under standard incubation conditions (Figure 2A). B88 cell shape did not change when treated with cetuximab (Figure 2B); when treated with 4-PBA, B88 changed from an epithelial sheet-like structure to a spindle shape (Figure 2C). B88

cells showed marked changes and exhibited signs of cellular damage when treated with 4-PBA and cetuximab, including disruption of the intercellular junction complexes, swollen or prominent nuclei, shrunken cytosol, ruptured nuclear and plasma membranes, or nuclear fragmentation (Figure 2D).

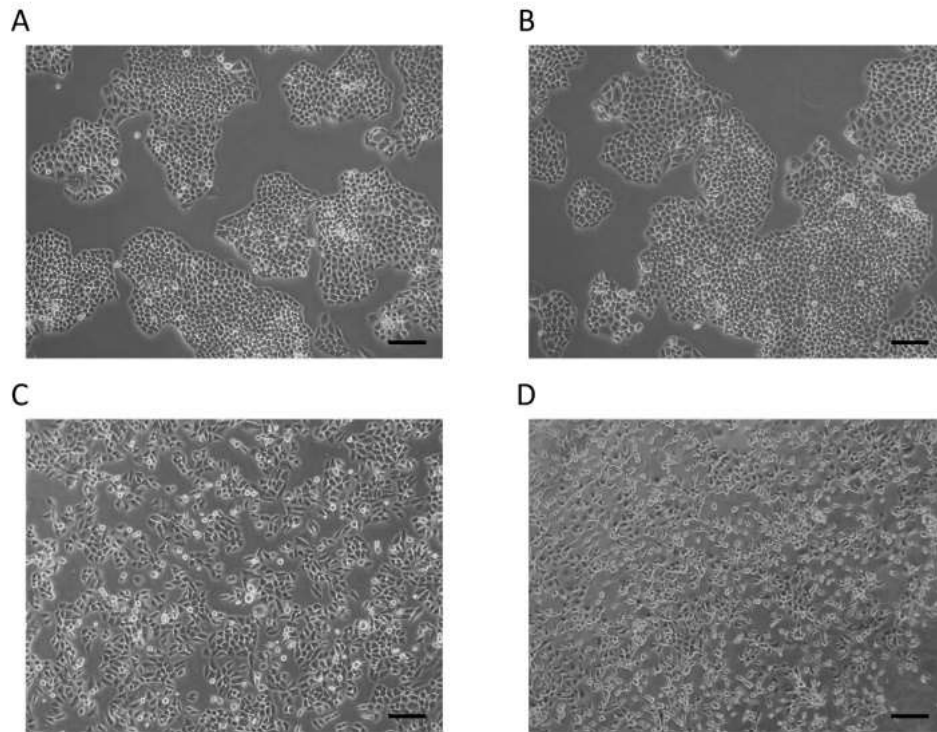


Figure 2: 4-PBA caused a significant effect in morphology. B88 cells were treated with cetuximab and/or 4-PBA for 24 h. When treated with cetuximab, B88 had not changed (A, B). When treated with 4-PBA, B88 had changed shape from epithelial sheet-like structure to spindle shape (C). When treated with 4-PBA and cetuximab, B88 had changed markedly (D). Scale bars, 100 μ m.

3.3 The mRNA levels of EGFR were elevated after treatment with 4-PBA

Treatment of B88 cells with cetuximab for 24 h significantly reduced EGFR mRNA expression by ~50% (Figure 3). Treatment of B88 cells with 4-PBA slightly

increased EGFR mRNA expression. Interestingly, treatment of B88 cells with a combination of 4-PBA and cetuximab increased EGFR mRNA expression. It is evident from these findings that the mRNA levels of EGFR are affected by 4-PBA treatment.

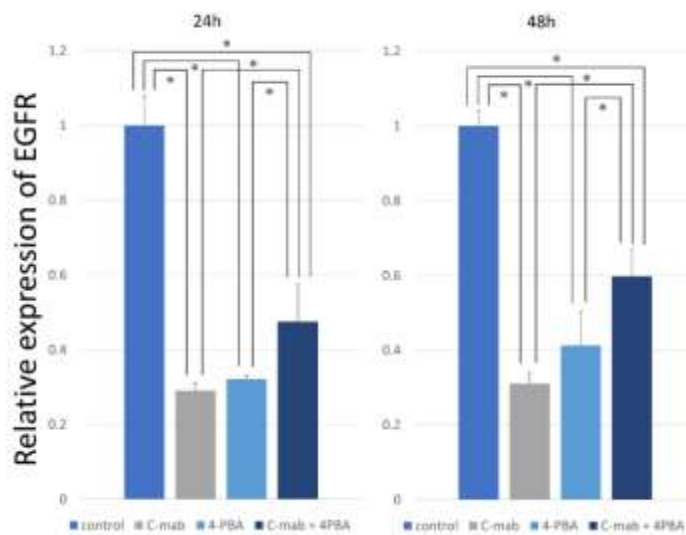


Figure 3: Expression analysis of EGFR. B-88 cells were treated with cetuximab and/or 4-PBA for 24 h and 48h. The amount of targeted EGFR gene was determined by quantitative real-time PCR with normalization to GAPDH. The relative amount of EGFR gene was determined using the $2^{-\Delta\Delta Ct}$ method. When treated with cetuximab, EGFR expression was markedly decreased. When treated with 4-PBA and cetuximab, EGFR expression was increased. Values represent the mean \pm SD of three independent experiments * $p < 0.05$.

3.4 Mechanism of cetuximab/4-PBA-induced cell death

B88 cell viability, cytotoxicity, and apoptosis were measured using an ApoToxGlo Triplex Assay to further evaluate the effects of cetuximab/4-PBA. The 4-PBA treatment resulted in a dose-dependent reduction in the number of viable B88 cells (Figure 4A), and cell toxicity was

increased (Figure 4B). In addition, treatment with different concentrations of 4-PBA (0.31, 0.62, 1.25, 2.5, 5.0, 10 mM) resulted in activation of caspase 3/7 (Figure 4C). These results indicate that 4-PBA increased cetuximab-induced cell toxicity and apoptosis in a dose-dependent manner.

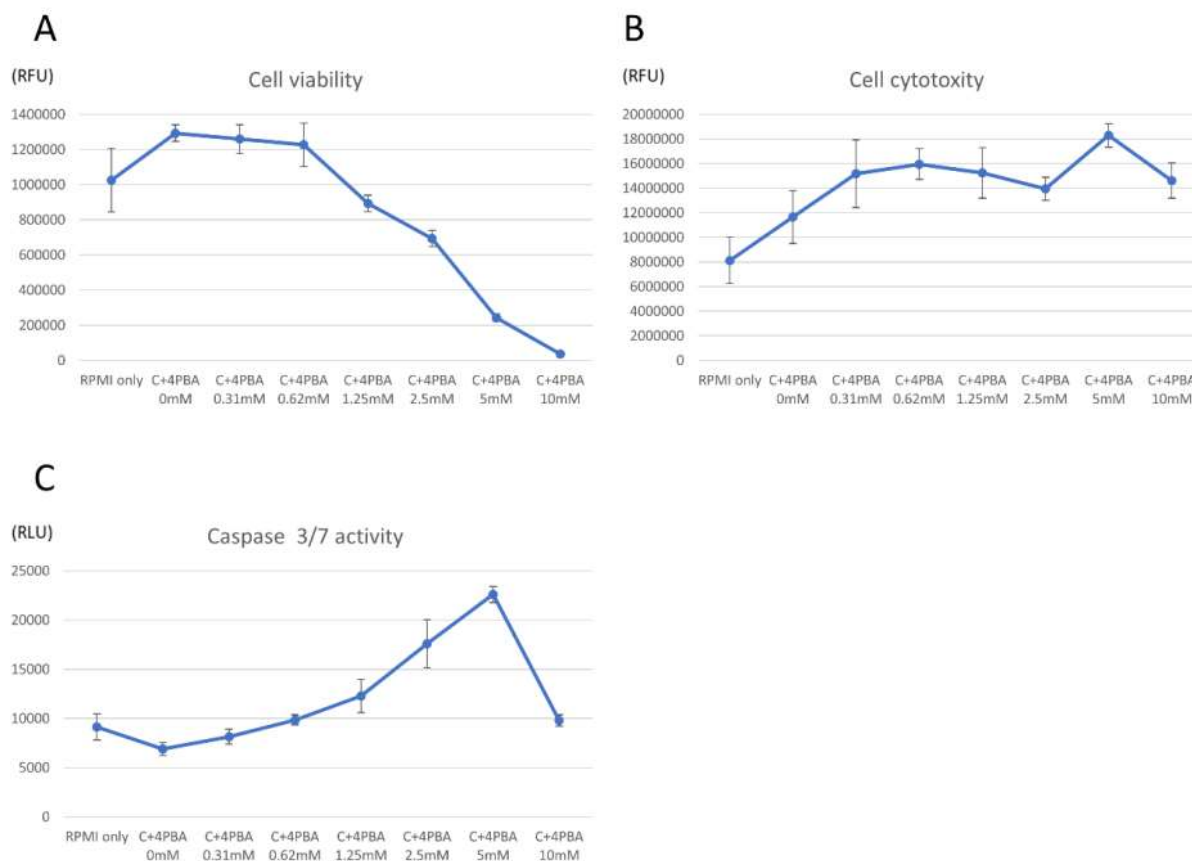


Figure 4: *In vitro* viability, cytotoxicity and caspase activity were dependent upon dosage of 4-PBA. B88 cells were cultured and treated with 4-PBA in 96-well format at the indicated doses for 24 h to measure the cellular viability, cytotoxicity and caspase activity using the ApoTox-Glo assay. B88 cells in suspension were treated with 4-PBA resulting in a dose-dependent decrease in cell viability (A) and concomitantly increase in cell cytotoxicity (B) and caspase-3/7 activation (C), which were consistent with apoptosis. Values represent the mean \pm SD of three independent experiments.

3.5 Effects of the treatment with the combination of cetuximab and 4-PBA on apoptosis

We performed TUNEL staining to investigate the effects of the treatment with the combination of cetuximab and 4PBA on B88 cell apoptosis. We observed only a few apoptotic cells in the control group and cetuximab-treated group (Figure 5A, B and E); apoptosis was slightly increased following treatment of B88 with 4-PBA (Figure 5C and E). The most substantial increase in apoptosis was observed in

the combination treatment group (Figure 5D and E). To further investigate the effects of the combination treatment with cetuximab and 4-PBA on apoptosis, the expression levels of CHOP, PERK Bcl-2, and PARP were examined by western blot analysis (Figure 6A). Our results indicated that the expression levels of CHOP, PERK, and Bcl-2 were decreased and that cleaved-PARP was increased in the combination treatment group.

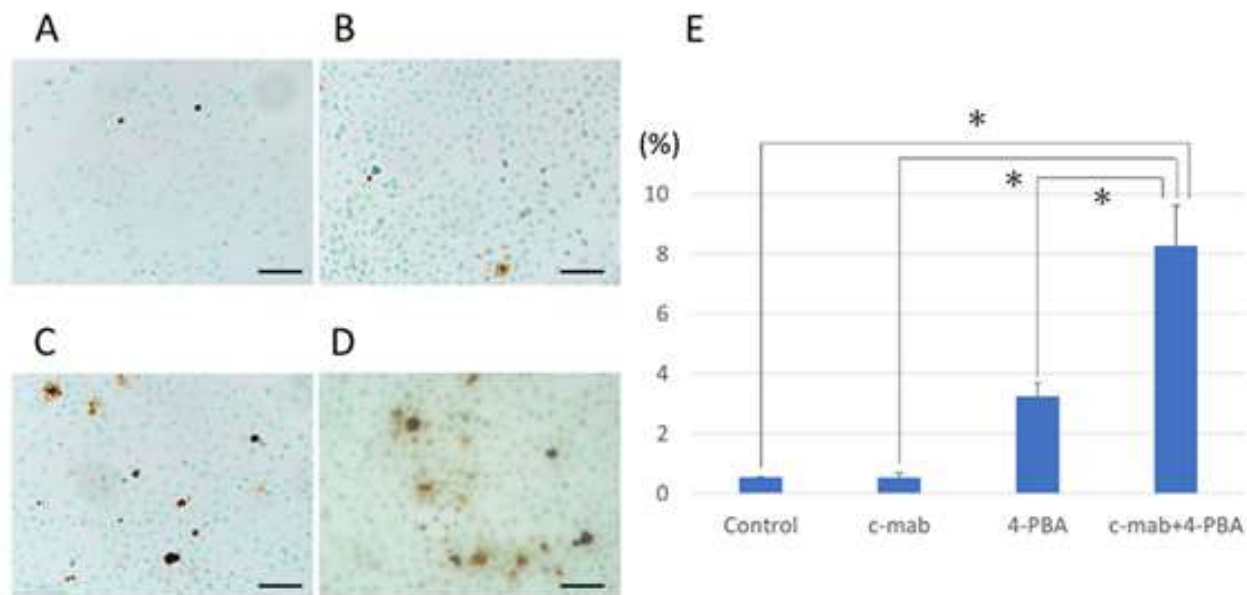


Figure 5: TUNEL assay to determine 4-PBA-induced apoptosis of B88 cells. TUNEL assay was used to confirm the induction of apoptosis in cetuximab and/or 4-PBA treated cells. (A) control, (B) c-mab, (C) 4-PBA, (D) c-mab + 4-PBA treated cells were confirmed by the appearance of TUNEL-positive cells. Scale bars, 50 μ m. (E) Results were quantified as the percentage of TUNEL-positive cells in 4 high magnification fields per slide. Values represent the mean \pm SD of three independent experiments. * p <0.05

3.6 Combination of cetuximab and 4-PBA activates mitogen-activated protein kinase /ERK pathway

EGFR signaling is transduced by two main pathways mediated by the PI3K-Akt and RAS-RAF-MEK-MAPK. To determine whether phosphorylation of EGFR induced by either 4-PBA or cetuximab is accompanied by activation

of these pathways, we examined the levels of phosphorylated Akt and ERK. Treatment with cetuximab alone did not change the levels of phosphorylated/total Akt and ERK (Figure 6B). Interestingly, treatment with 4-PBA upregulated the expression of phosphorylated ERK. In contrast, the levels of Akt did not change.

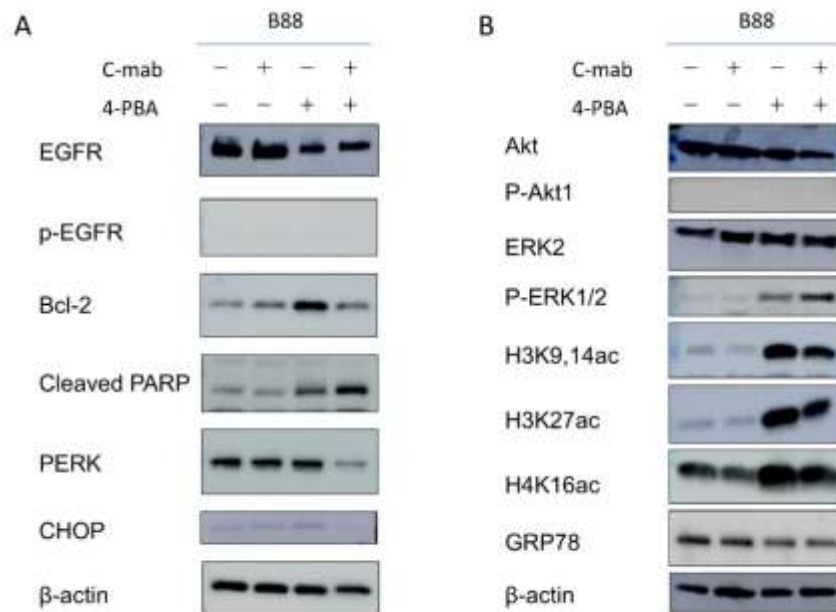


Figure 6: Western blotting after treatment with cetuximab and/or 4-PBA in B88 cells. Western blot analyses for apoptosis-related molecules and related pathways were performed. (A) Western blotting for apoptosis-related molecules after treatment. The expression levels of CHOP, PERK and Bcl-2 were decreased. The expression level of cleaved PARP was elevated by the treatment. (B) Western blotting for related pathways after treatment. The phosphorylation level of AKT was not changed. In contrast, the phosphorylation of ERK1/2 was increased by the 4-PBA treatment. The levels of H3K9/27ac, H3K14,27ac and H4K16ac were increased, GRP78 was decreased by the 4-PBA treatment. β-actin was used as an internal control.

3.7 Combination of cetuximab and 4-PBA modulates histone acetylation and ER stress in B88 cells

Histone acetylation level is a widely accepted marker for HDAC inhibition. For this reason, we examined the HDACi activity of 4-PBA in OSCC cells. Western blot analysis showed that 4-PBA treatment of B88 cells induced histone H3K9, H3K14, 27, and H4K16 acetylation. The levels of H3K9ac, H3K14ac, 27ac, and H4K16ac were increased (Figure 6B), indicating that the acetylation of H3 might play an important role in promoting EGFR gene transcription [14, 15]. Furthermore, we investigated

whether 4-PBA could promote the EGFR signaling pathway. The results showed that 4-PBA significantly increased phosphorylation levels of phospho-ERK. The combination of cetuximab and 4-PBA further increased the expression. Interestingly, protein levels of the ER stress marker, GRP78, were significantly decreased in 4-PBA treated and combination of cetuximab and 4-PBA cells, but not in cetuximab only treated cells (Figure 6). These data also show that histone H3 hyperacetylation may correlate with ER stress.

4. Discussion

We screened the candidate materials for repurposing and/or repositioning of cetuximab in commercially available drugs and found that 4-PBA had the potential to induce apoptosis and upregulate the EGFR signaling pathway in OSCC cells. The role of 4-PBA has been established as an alleviator of ER stress. In addition, 4-PBA has antitumor activity as an HDACi. HDACi are divided into different classes based on their chemical properties, including hydroxamic acids, such as suberoylanilide hydroxamic acid (SAHA), trichostatin A; short chain fatty acids, such as 4-PBA and valproic acid; cyclic tetrapeptides, such as apicidin and depsipeptide (also known as FK228 or romidepsin); and benzamides [16, 17]. The varying action of 4-PBA with different HDACi is what improves ER stress. 4-PBA is a histone deacetylase inhibitor and a short-chain fatty acid chemical chaperon that stabilizes protein conformation, improves the capacity of ER folding, and facilitates proper trafficking of mutant proteins. Additionally, 4-PBA acts as an ammonia scavenger in patients with urea cycle disorders and hyperammonemia [18]. Subsequently, it has been shown that inhibition of the autophagy-mediated lipotoxic state causes increased cytosolic calcium levels [19]. It has also been demonstrated that 4-PBA inhibits tumor growth and epithelial–mesenchymal transition of human OSCC cells [20]. In this study, as expected from earlier research, 4-PBA prevented ER stress and histone deacetylation, and increased the expression of EGFR. It is also worth noting that cetuximab treatment with 4-PBA induced apoptosis and increased the expression of phospho-ERK in OSCC cells.

The mitogen-activated protein kinase (MAPK) signaling pathway plays a central role in the regulation of gene

expression, cellular growth, and survival [21]. Defects in the MAPK/ERK pathway lead to uncontrolled cell growth, a necessary step for the development of cancer [22]. Therefore, many researchers have suggested the role of ERK signaling activation in delivering a survival signal that counteracts proapoptotic signaling such as p38. ERK inhibitors have demonstrated preliminary antitumor activity and may be most effective against cancers with RAS, RAF, or MAPK pathway alterations. Several ERK inhibitors (BVD-523, GDC-0994, CC-90003, *etc.*) have been approved by the Food and Drug Administration for advanced solid tumors [23]. In contrast, some studies in other organs have provided insights into the correlation between ERK activation and anticancer effects [24]. Depending on the cell type and stimulus, ERK activity will mediate different antiproliferative events, such as apoptosis. Satoh *et al.* [25] showed that acetoxychavicol acetate-28 (ACA-28) strongly stimulated ERK phosphorylation in melanoma cells. Consequently, ACA-28 specifically induced apoptosis that was abrogated when ERK activation was blocked with the specific MEK inhibitor U0126. There is a possibility that the induction of epigenetic alteration by 4-PBA affects the apoptosis linked to stimulation of oncogenic signaling, such as the MAPK/ERK pathway. Contrary to our findings, Shi *et al.* [26, 27] showed that 4-PBA promotes the migration of gastric cancer cells through upregulation of HER3/HER4, subsequent to increased levels of acetyl-histone and activation of ERK signaling. The results of the present study do show that 4-PBA significantly increased phosphorylation levels of phospho-ERK. However, these studies do not adequately account for the significant inhibition of gastric cancer cell proliferation in the presence of 4-PBA concentrations of 5 mM or above; therefore, the potential for antitumor effects seem to be lacking.

The present study clearly shows that the combination of 4-PBA and cetuximab upregulates phosphorylated ERK expression, although cell viability decreases and apoptosis increases. ER stress-induced apoptosis can be triggered via different pathways. CHOP plays an important role in ER stress-induced apoptosis [28]. CHOP is a transcription factor that positively promotes apoptosis following PERK activation. In this study, 4-PBA induced ER stress that was not evidenced by an increase in PERK and CHOP. Rather, the expression of PERK and CHOP in cells treated with 4-PBA and cetuximab was importantly attenuated. Taken together, these data suggest that 4-PBA induces apoptosis by triggering the EGFR signaling pathway. One of the limitations of this study is the discrepancy between mRNA and protein expression of EGFR in the combination treatment. The mRNA expression of EGFR increased in the combination treatment; however, the protein level of EGFR remained unchanged. Our results suggest a posttranscriptional modulation of EGFR expression. This may contribute to the activation of ERK. A further study of this phenomenon should be conducted.

5. Conclusions

In summary, we demonstrated that cetuximab with 4-PBA induced histone acetylation and/or ER stress responses in OSCC cells, providing novel insights into the 4-PBA-mediated enhancement of antitumor activity by cetuximab. One interpretation of our results is that the EGFR signaling pathway is not affected by the accumulation of aberrant epigenetic alterations in oral cancer cells. It is clear that histone modification and/or ER stress prevents the action of cetuximab. Thus, therapeutic intervention using a chemical chaperon (4-PBA) that stabilizes misfolded proteins could provide a promising strategy for the enhancement of antitumor activity by cetuximab. Our findings provide

experimental evidence for the application of combination therapy in the clinical treatment of OSCC. We hope the findings presented in this paper will contribute to a better understanding of the mechanisms of action of cetuximab.

Acknowledgments

The Authors would like to thank A. Shimomura for technical assistance with the experiments. The Authors would also like to thank Editage (www.editage.com) for English language editing.

Conflicts of Interest

The authors declare no conflict of interest.

References

1. Jiang X, Wu J, Wang J, et al. Tobacco and oral squamous cell carcinoma: A review of carcinogenic pathways. *Tob Induc Dis* 17 (2019): 29.
2. El-Naggar JKCC AK, Grandis JR, Takata T, et al. WHO Classification of Head and Neck Tumours. 4th ed. Lyon, France: IARC (2017).
3. Ryott M, Wangsa D, Heselmeyer-Haddad K, et al. EGFR protein overexpression and gene copy number increases in oral tongue squamous cell carcinoma. *Eur J Cancer* 45 (2009): 1700-1708.
4. Dutta PR, Maity A. Cellular responses to EGFR inhibitors and their relevance to cancer therapy. *Cancer Letters* 254 (2007): 165-177.
5. Lievre A, Bachet JB, Le Corre D, et al. KRAS mutation status is predictive of response to cetuximab therapy in colorectal cancer. *Cancer Res* 66 (2006): 3992-3995.
6. Lievre A, Laurent-Puig P. Genetics: Predictive value of KRAS mutations in chemoresistant CRC. *Nat Rev Clin Oncol* 6 (2009): 306-307.

7. Wheeler DL, Dunn EF, Harari PM. Understanding resistance to EGFR inhibitors-impact on future treatment strategies. *Nat Rev Clin Oncol* 7 (2010): 493-507.
8. Lui VW, Hedberg ML, Li H, et al. Frequent mutation of the PI3K pathway in head and neck cancer defines predictive biomarkers. *Cancer Discov* 3 (2013): 761-769.
9. Tasoulas J, Giaginis C, Patsouris E, et al. Histone deacetylase inhibitors in oral squamous cell carcinoma treatment. *Expert Opinion on Investigational Drugs* 24 (2015): 69-78.
10. Haigentz M, Kim M, Sarta C, et al. Phase II trial of the histone deacetylase inhibitor romidepsin in patients with recurrent/metastatic head and neck cancer. *Oral Oncology* 48 (2012): 1281-1288.
11. Shen J, Huang C, Jiang L, et al. Enhancement of cisplatin induced apoptosis by suberoylanilide hydroxamic acid in human oral squamous cell carcinoma cell lines. *Biochem Pharmacol* 73 (2007): 1901-1909.
12. Erlich RB, Rickwood D, Coman WB, et al. Valproic acid as a therapeutic agent for head and neck squamous cell carcinomas. *Cancer Chemotherapy and Pharmacology* 63 (2009): 381-389.
13. Uchida D, Begum N-M, Almofti A, et al. Possible role of stromal-cell-derived factor-1/CXCR4 signaling on lymph node metastasis of oral squamous cell carcinoma. *Experimental Cell Research* 290 (2003): 289-302.
14. Cheung P, Tanner KG, Cheung WL, et al. Synergistic Coupling of Histone H3 Phosphorylation and Acetylation in Response to Epidermal Growth Factor Stimulation. *Molecular Cell* 5 (2000): 905-915.
15. Yang W, Xia Y, Hawke D, et al. PKM2 Phosphorylates Histone H3 and Promotes Gene Transcription and Tumorigenesis. *Cell* 150 (2012): 685-696.
16. Xu WS, Parmigiani RB, Marks PA. Histone deacetylase inhibitors: molecular mechanisms of action. *Oncogene* 26 (2007): 5541-5552.
17. Mai A, Altucci L. Epi-drugs to fight cancer: From chemistry to cancer treatment, the road ahead. *The International Journal of Biochemistry & Cell Biology* 41 (2009): 199-213.
18. Brusilow SW. Phenylacetylglutamine may replace urea as a vehicle for waste nitrogen excretion. *Pediatr Res* 29 (1991): 147-150.
19. Iannitti T, Palmieri B. Clinical and experimental applications of sodium phenylbutyrate. *Drugs R D* 11 (2011): 227-249.
20. Qian K, Sun L, Zhou G, et al. Sodium Phenylbutyrate Inhibits Tumor Growth and the Epithelial-Mesenchymal Transition of Oral Squamous Cell Carcinoma In Vitro and In Vivo. *Cancer Biother Radiopharm* 33 (2018): 139-145.
21. Zhang W, Liu HT. MAPK signal pathways in the regulation of cell proliferation in mammalian cells. *Cell Research* 12 (2002): 9-18.
22. Downward J. Targeting RAS signalling pathways in cancer therapy. *Nature Reviews Cancer* 3 (2003): 11-22.
23. Chin HM, Lai DK, Falchook GS. Extracellular Signal-Regulated Kinase (ERK) Inhibitors in Oncology Clinical Trials. *Journal of Immunotherapy and Precision Oncology* 2 (2020): 10-16.
24. Cagnol S, Chambard J-C. ERK and cell death: Mechanisms of ERK-induced cell death – apoptosis, autophagy and senescence. *The FEBS Journal* 277 (2010): 2-21.

25. Satoh R, Hagihara K, Matsuura K, et al. Identification of ACA-28, a 1'-acetoxychavicol acetate analogue compound, as a novel modulator of ERK MAPK signaling, which preferentially kills human melanoma cells. *Genes to Cells* 22 (2017): 608-618.
26. Shi X, Zheng C, Li C, et al. 4-Phenybutyric acid promotes gastric cancer cell migration via histone deacetylase inhibition-mediated HER3/HER4 up-regulation. *Cell Biology International* 42 (2018): 53-62.
27. Shi X, Gong L, Liu Y, et al. 4-phenylbutyric acid promotes migration of gastric cancer cells by histone deacetylase inhibition-mediated IL-8 upregulation. *Epigenetics* 15 (2020): 632-645.
28. Hu H, Tian M, Ding C, et al. The C/EBP Homologous Protein (CHOP) Transcription Factor Functions in Endoplasmic Reticulum Stress-Induced Apoptosis and Microbial Infection. *Frontiers in Immunology* 9 (2019).



This article is an open access article distributed under the terms and conditions of the [Creative Commons Attribution \(CC-BY\) license 4.0](https://creativecommons.org/licenses/by/4.0/)